PHYSICAL REVIEW A VOLUME 35, NUMBER 6 MARCH 15, 1987

Homoclinic explosion in the vicinity of bifurcation at the triple-zero eigenvalue

L. M. Pismen
Department of Chemical Engineering, Technion-Israel Institute of Technology, Haifa 32000, Israel
(Received 28 January 1986; revised manuscript received 2 September 1986)

Equations describing small-amplitude motion in the proximity of bifurcation at the triple-zero eigenvalue, after being reduced to a normal form by nonlinear transformations, display a double-scale structure that combines relatively fast conservative orbital motion with slow dissipative evolution of two integrals of motion. The homoclinic explosion occurs when the attractor of the averaged dissipative equations comes close to a homoclinic trajectory of the fast conservative subsystem. Applying the method of matched asymptotic expansions allows one to reduce the dynamical system near this point to a simple next return map possessing an infinite family of invariant manifolds that can turn into attractors of different character under small parametric perturbation. After the attractor of the averaged system has been expelled from the region of closed orbits, one observes large-amplitude dynamics with rare events of anomalous intermittency superimposed upon a quasiperiodic or chaotic attractor of nonuniversal character.

I. INTRODUCTION

The vicinity of a bifurcation at the triple-zero eigenvalue is a natural place to look for different types of chaotic regimes and routes to chaos in dynamical systems. One can expect to encounter there a large variety of behavior characteristic to three-dimensional motion, in the same way as all kinds of two-dimensional phase portraits are observed near a bifurcation at the double-zero eigenvalue.[1] This host of behaviors would be tightly packed into a narrow parametric patch near the singular point, and dynamics scaled down to small-amplitude motions more amenable to analytical study.

Derivation of normal forms and studies of dynamics near the bifurcation at the triple-zero eigenvalue have been reported by Arneodo *et al.*[2] with the specific application to the triple-diffusive Benard convection problem. Normal forms are insensitive to details of an underlying physical problem, being dependent only on its symmetry (for example, quadratic terms are excluded in Ref. 2 due to special symmetry properties of the Benard problem in the Boussinesq approximation). The resulting universality, allowing one to describe systems of different physical origin by the same set of amplitude equations of relatively simple structure, is marred, however, by a purely technical difficulty: equations displaying a rich variety of solutions turn out themselves to be complex enough to require numerical integration, thus losing much of their appeal.

The prospects would improve substantially if an additional small parameter finds its way into amplitude equations. This, in fact, can happen in a quite natural way. Generically, the degeneracy has to be geometrical as well as algebraic, and the scaling of the projection on the only eigenvector can be different from that of projections on other vectors spanning the invariant subspace. This scaling property manifests itself quite clearly in a hierarchy of amplitude equations corresponding to the hierarchy of singular bifurcations of increasing codimension at the double-zero eigenvalue.[3] Members of this hierarchy possess a double-scale structure combining rapid conservative motion with dissipative motion on a slower time scale.

As we shall presently see, a similar double-scale structure manifests itself in amplitude equations describing dynamics in the proximity of a bifurcation at the triple-zero eigenvalue combined with the cusp singularity of stationary solutions. The codimension of this bifurcation is four; nevertheless, it is in no way exotic, and can be detected, e.g., in a system as simple as a combination of consecutive exothermic and endothermic chemical reactions in a stirred vessel or a single exothermic reaction with an external capacitor.[4]

An attractive feature of cusp singularity (that a generic bifurcation at the zero eigenvalue does not possess) is the possibility to consider the region of small amplitudes as the only attractor of the underlying system. This is demonstrably so in simple cases when there are no more than three stationary states and the underlying physics rules out the escape of trajectories to infinity.

Detecting chaotic dynamics is our main purpose. Separation of characteristic scales of the conservative and dissipative motion, allowing the use of orbital averaging, is the property that makes the problem tractable. We shall pay most attention to the behavior in the proximity of homoclinic orbits of the truncated (conservative) system. When trajectories of the averaged system cross the locus of these orbits one can observe a peculiar intermittency phenomenon described by Fowler,[5] superimposed on a large-amplitude quasiperiodic or chaotic attractor of nonuniversal character. The analytically tractable small-amplitude chaos is to be detected under conditions when the attractor of the averaged equations comes close to the locus of homoclinic orbits. Using the method of matched asymptotic expansions we derive for this case an approximate next-return map (similar to the area-preserving Chirikov map[6]) that generates a complex structure of orbits with repeated period N-tupling in resonance regions.

II. TRANSFORMATION TO THE NORMAL FORM

Suppose that the dynamical system has been reduced by projecting on a suitable basis in the three-dimensional ker-

nel space to the form

$$\dot{\mathbf{u}}=L\mathbf{u}+\mathbf{f}(\mathbf{u}) , \tag{1}$$

where L is the normal Jordan block

$$L=\begin{vmatrix}0&1&0\\0&0&1\\0&0&0\end{vmatrix} \tag{2}$$

and $\mathbf{f}(\mathbf{u})$ vanishes at the origin together with its first derivatives. Generically, only quadratic terms in $\mathbf{f}(\mathbf{u})$ need to be retained near the origin. Applying a nonlinear transformation

$$\mathbf{u}=\mathbf{v}+\mathbf{p}(\mathbf{v}) \tag{3}$$

with an appropriately chosen quadratic form $\mathbf{p}(\mathbf{v})$ reduces the quadratic part of Eq. (1) to any out of 14 equivalent normal forms (see the Appendix). Choosing a most convenient one, and dropping cubic and higher-order terms, we rewrite the transformed Eq. (1) as

$$\dot{x}=y,\ \ \dot{y}=z,\ \ \dot{z}=\mu_0x^2+\mu_1xy+\mu_2y^2+\mu_3xz . \tag{4}$$

Adding a cubic term would be necessary for retaining the structural stability in a singular case when one of the coefficients μ_i happens to vanish. The case $\mu_0=0$, when the cubic term νx^3 should be added, is of particular interest, since it corresponds to the cusp singularity of stationary solutions to Eq. (1) or (4). The advantage of this case is that a cubic form with $\nu<0$, unlike the quadratic form (4), prevents the escape of trajectories to infinity; thus, a cubic form can represent realistic global dynamics of a physical system. Further on, we restrict attention to this case and replace the last of Eq. (4) by

$$\dot{z}=\mu_1xy+\mu_2y^2+\mu_3xz+\nu x^3 . \tag{5}$$

The unfolding of Eq. (5) obtained by allowing for small deviations of parameters from the singular point is

$$\dot{z}=\kappa+\lambda_1x+\lambda_2y+\lambda_3z+\mu_1xy+\mu_2y^2+\mu_3xz+\nu x^3 . \tag{6}$$

Four constants κ,λ_i depending on parametric deviations are necessary and sufficient for constructing a universal unfolding of the codimension-four bifurcation under the study.

Order-of-magnitude considerations can be invoked at this stage. The lowest-order form (4) or (6) can replace the original system (1) only near the origin, say, at $x=O(\epsilon)$. Then Eq. (5) can be balanced only if the dynamics unfolds on a slow time scale extended by the factor $O(\epsilon^{-1/2})$ so that $y=O(\epsilon^{3/2})$, $z=O(\epsilon^2)$, and both $\dot{z}$ and xy in Eq. (5) are $O(\epsilon^{5/2})$ while other terms in this equation are $O(\epsilon^3)$. We shall assign the following orders of magnitude of parametric deviations: $\kappa=O(\epsilon^3)$, $\lambda_1=O(\epsilon^2)$, $\lambda_2=O(\epsilon)$, $\lambda_3=O(\epsilon)$. This choice, defining the neighborhood of the singular point in the parametric space where the following analysis is applicable, is not unique. One can see, however, that it engenders the greatest possible variety of behavior by balancing the orders of magnitude of terms dependent on parametric deviations, on one hand, and corresponding higher-order terms, on another. Rescaling to $O(1)$ variables ($x\to\epsilon x$, etc.) we obtain finally

$$\dot{x}=y,\ \dot{y}=z ,$$
$$\dot{z}=(\alpha+x)y+\epsilon^{1/2}(\kappa+\beta x-x^3+\gamma z+ay^2+bxz) . \tag{7}$$

The coefficient at xy has been reduced to unity by rescaling; in addition, the time scale can be chosen to reduce α to ±1. The remaining italic parameters (a,b) in Eq. (7) are defined by the underlying system (1) while those denoted by Greek characters depend on parametric deviations.

III. WEAKLY DISSIPATIVE DYNAMICS

Equation (7) truncated at $\epsilon=0$ and rewritten as

$$\dddot{x}+x\dot{x}-\alpha\dot{x}=0 \tag{8}$$

is recognized as a traveling-wave form of the Korteweg–de Vries equation. This equation has a continuous family of stationary states $x=q$, $y=z=0$ with arbitrary q, and possesses two integrals of motion:

$$K=z-\alpha x-\tfrac{1}{2}x^2 ,$$
$$H=\tfrac{1}{2}y^2-xz+\tfrac{1}{2}\alpha x^2+\tfrac{1}{3}x^3 . \tag{9}$$

The eigenvalues of Eq. (8) linearized near the branch of stationary points are 0 and $\pm(q+\alpha)^{1/2}$. At $q>-\alpha$, the stationary point has a one-dimensional stable and a one-dimensional unstable manifold, in addition to the one-dimensional center manifold directed along the locus of stationary points in the three-dimensional phase space (x,y,z). At $q<-\alpha$, the stationary point has a three-dimensional center manifold. To underline this distinction, we shall call stationary points at $q>-\alpha$ and $q<-\alpha$, respectively, hyperbolic and elliptic.

In addition to the family of stationary states, Eq. (8) possesses a continuous two-parametric family of orbits parametrized by the integrals K,H. If

$$K=K_0=-q(\alpha+\tfrac{1}{2}q),\ \ H=H_0=q^2(\tfrac{1}{2}\alpha+\tfrac{1}{3}q) , \tag{10}$$

and $q<-\alpha$, the integral curve (9) collapses into a single (elliptic) point $x=q$, $y=z=0$. If, again, Eq. (10) holds but $q>-\alpha$, Eq. (9) defines a homoclinic trajectory passing through the (hyperbolic) point $x=q$, $y=z=0$. The branches of elliptic and hyperbolic points meet in a cusp at $q=-\alpha$ (Fig. 1). Closed orbits exist at K,H within the region between the elliptic and hyperbolic branches in Fig. 1, while outside this region integral curves are unbounded.

At $\epsilon\neq0$, both integrals evolve on an extended time scale:

$$\dot{K}=\epsilon^{1/2}G(x,y,z),\ \ \dot{H}=-x\dot{K} , \tag{11}$$

where $G(x,y,z)=\kappa+\beta x-x^3+\gamma z+ay^2+bxz$ is the "dissipative" function in Eq. (7).

Since H,K evolve on a slow time scale, the right-hand sides of Eq. (11) can be approximated by corresponding orbital averages:

$$\epsilon^{-1/2}\dot{K}=\langle G(x,y,z)\rangle ,$$
$$\epsilon^{-1/2}\dot{H}=-\langle xG(x,y,z)\rangle . \tag{12}$$

To compute the averages $\langle\ \rangle$, we define orbits $y(x;K,H)$,

$z(x;K,H)$ using Eq. (9):

$$z=K+\alpha x+\tfrac{1}{2}x^2\ ,$$
$$y=\sqrt{2}(H+Kx+\tfrac{1}{2}\alpha x^2+\tfrac{1}{6}x^3)^{1/2} \tag{13}$$

and replace time averages by averages along half-orbits, e.g.,

$$\langle G\rangle=\frac{1}{T}\int_0^T G(x(t),y(t),z(t))dt$$
$$=\frac{2}{T}\int_{x_-}^{x_+} y^{-1}\hat{G}(x;H,K)dx\ , \tag{14}$$

where $\hat{G}(x;H,K)=G(x,y(x,H,K),z(x,H,K))$. The period T can be computed, if needed, in a similar way as

$$T=2\int_{x_-}^{x_+}\frac{dx}{y(x)}\ . \tag{15}$$

The integration limits $x_\pm(K,H)$ are defined as the two smaller roots of the polynomial under the radical in Eq. (13). This polynomial has three real roots when K,H lie within the cusped region in Fig. 1.

Denoting the averages in Eq. (12) as $\langle G\rangle=F_0(H,K)$ and $\langle xG\rangle=F_1(H,K)$, and rescaling time by the factor $\epsilon^{1/2}$, we obtain, finally, the dynamic equations of H,K in the form

$$\dot{K}=F_0(H,K),\quad \dot{H}=F_1(H,K)\ . \tag{16}$$

An obvious stationary solution of this equation, corresponding to stationary points of Eq. (7), is given by $H_s=H_0(q_s)$, $K_s=K_0(q_s)$, where $q_s<-\alpha$ is a root of the cubic form $f(q)=\kappa+\beta q-q^3$ lying on the elliptic branch in Fig. 1. A stationary point $H=H_s,K=K_s$ satisfying $F_0(H_s,K_s)=F_1(H_s,K_s)=0$ corresponds to a periodic orbit of Eq. (7) when H_s,K_s lie within the cusped region in Fig. (3). The orbital averaging implied in Eq. (16) becomes invalid when H_s,K_s approach the homoclinic branch in Fig. 1, and Eq. (16) must be modified when the period of orbital motion increases to $T=O(\epsilon^{-1/2})$—see Sec. IV. Outside the cusped region in Fig. 1, where trajectories are unbounded, Eq. (16) is not applicable.

The functions $F_0(H,K),F_1(H,K)$ in Eq. (16) can be expressed through elliptic integrals. Stability conditions for steady orbits can be also obtained explicitly (albeit as awesome expressions generated by a symbolic computation program). In this way one can locate bifurcations of periodic orbits, and detect the emergence of invariant tori of Eq. (7) at Hopf bifurcation points of the averaged system (16).

Depending upon the values of the five parameters of the dissipative function $G(x,y,z)$, one can realize different phase portraits of Eq. (16). Two examples [both of which, as we shall see below indicate chaotic dynamics of the full system (7)] are given in Fig. 1. The averaged equations (16) are applicable at all times if this system has attractors (either stationary points or periodic orbits) within the cusped region in Fig. 1, including the elliptic but excluding the hyberbolic branch.

Looking for chaotic dynamics, one is naturally drawn to situations when homoclinic orbits can be detected in truncated or averaged equations. One can think of either

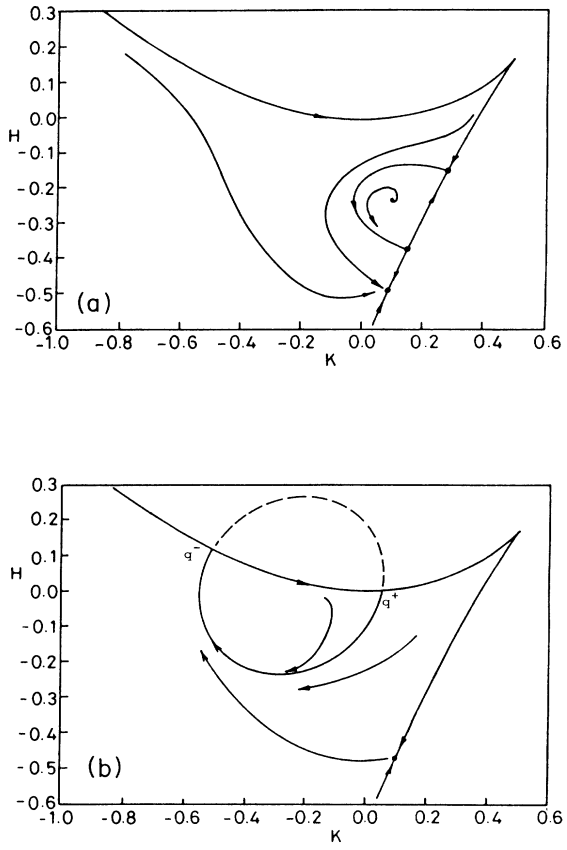

FIG. 1. The cusped region of closed orbits, with qualitatively drawn trajectories of the averaged system (12) corresponding to (a) formation of a homoclinic orbit of Eq. (12) and (b) escape to the region of unbounded orbits and reinjection.

the averaged system (16) possessing a homoclinic cycle or a trajectory of Eqs. (16) passing through a homoclinic orbit of Eq. (8) corresponding to $K=K_0$, $q>-\alpha$.

A simplest suitable homoclinic cycle of the averaged equations [Fig. 1(a)] would involve two stationary states $x=q_1,q_2$ with $q_1<\gamma/b<q_2<-\alpha$, $q_1^2>\beta/3>q_2^2$. These conditions ensure that both points lie on the elliptic branch of Eq. (11) and are saddles when viewed as stationary points of Eq. (16). Existence of chaotic trajectories of the full system (7) near such a homoclinic cycle is by now a standard feature that has been detected in studies of the codimension-two bifurcation at zero and imaginary eigenvalues (sometimes called the Melnikov bifurcation[1]). We refer to Ref. 7 for detailed studies of motion near homoclinic orbits of this type.

Chaos associated with homoclinic orbits similar to that in Fig. 1(a) is strictly confined in the parametric space of Eq. (7), though it might carry on in the parametric space of the underlying system well away from the codimension-four singularity under study. Note also that under these conditions Eq. (16) should possess another attractor, and the chaotic orbit may well "leak," i.e., represent in fact a long transient.

IV. MOTION ACROSS THE HYPERBOLIC BRANCH

Further on, we shall concentrate on another possible source of chaos that appears when dynamics generated by Eq. (16) brings trajectories of the averaged system to and beyond the hyperbolic branch in Fig. 1. The case when orbits undergo a qualitative change during the slow evolution described by averaged equations was studied in another context by Shimizu and Ichikawa[8] and Fowler.[5] This qualitative change occurs when the trajectory of averaged equations crosses the locus of homoclinic orbits as in Fig. 1(b). In the vicinity of the hyperbolic branch, the orbital averaging is no longer justified by the separation of the scales of the orbital motion, on one hand, and of the evolution of the integrals H,K, on another. The continuous system (16) should be replaced under these conditions by a discrete system connecting values of H,K after each consecutive return into the vicinity of a saddle point of Eq. (7)—see Sec. V. The evolution becomes then very sensitive to occasional close approaches to the exact position of the homoclinic orbit; that leads to the peculiar intermittency phenomenon described by Fowler.[5]

We shall now examine in more detail motion in the proximity of the hyperbolic branch of Eq. (10). For this purpose, it is convenient to replace K,H by the variables $q=\frac{1}{2}(x_1+x_2)$, $p=\frac{1}{4}(x_1-x_2)^2$ where x_1,x_2 are the two largest real roots of the cubic form $x^3+3\alpha x^2+6Kx+6H$ (at $p>0$) or the complex-conjugate pair of roots (at $p<0$); $p=0$ corresponds to the hyperbolic branch of Eq. (10). Using

$$K=-q\left[\alpha+\frac{q}{2}\right]-\frac{p}{6},\quad H=(\tfrac{1}{2}+\tfrac{1}{3}q)(q^2-p)\ , \tag{17}$$

and denoting $\xi=q-x$, $r=\alpha+q$, reduces Eq. (11) to

$$\dot{p}=-2\epsilon^{1/2}[r^{-1}\xi G+O(p)]\ , \tag{18}$$

$$\dot{q}=-\epsilon^{1/2}[r^{-1}(1-\xi/3r)G+O(p)]\ . \tag{19}$$

At $p=O(\epsilon)$, $\xi=O(\epsilon^{1/2})$, motion along integral curves of the truncated system slows down, and, rather than averaging Eqs. (18) and (19), one has to solve this system together with the dynamic equation $\dot{x}=y$ from the full system (7). Rescaling the variables $p=\epsilon\phi$, $\xi=\epsilon^{1/2}\eta$, $q=q_0+\epsilon^{1/2}\psi$ and expressing y with the help of Eq. (13) yields, to the leading order,

$$\dot{\eta}=\dot{\psi}\pm[r_0(\eta^2-\phi)]^{1/2},\quad \dot{\psi}=-r_0^{-1}f_0\ ,$$
$$\dot{\phi}=-2r_0^{-1}\eta f_0\ , \tag{20}$$

where $f_0=f(q_0)=G(q_0,0,0)=\kappa+\beta q_0-q_0^3$, $r_0=\alpha+q_0$. It is convenient to integrate Eq. (20) with initial conditions $\phi=\phi^i$, $\psi=\psi^i,\eta=(\phi^i)^{1/2}$ set at the turning point where $y=[r_0(\eta^2-\phi)]^{1/2}$ vanishes; respectively, the upper and lower signs in Eq. (20) and below correspond to the outgoing and incoming branches of the trajectory. The integral curves of Eq. (20) are obtained in the form

$$\eta^2=\phi+c^2(\phi-\phi^i)^2\ , \tag{21}$$

$$\psi=\psi^i+\frac{1}{2c}\ln\frac{2|c|\eta\pm(\mathrm{sgn}c)[1+4c^2(\eta^2-\phi^i)]^{1/2}}{1+2|c|(\phi^i)^{1/2}}\ , \tag{22}$$

where $c=r_0^{3/2}/2f_0$. Admissible initial conditions are bounded by $\phi^i>\phi_c=1/4c^2$; otherwise the turning point does not exist. At $\phi^i=\phi_c$, η touches zero as ϕ dips to $\phi=-\phi_c$ either on the outgoing (at $c>0$) or on the incoming (at $c<0$) branch of the trajectory. The passage time diverges logarithmically at $\phi^i\to\phi_c$, so that q is ejected from the vicinity of q_0 when $\phi^i-\phi_c$ is *transcendentally* small.

We see that $-\epsilon\phi_c=-\epsilon/4c^2$ is the minimal value of p that still allows motion along a closed trajectory. At more negative p, the turning point does not exist, and the trajectories are unbounded. Note that p changes only by an $O(\epsilon)$ increment during the slow phase of the orbital motion, i.e., at $\xi=O(\sqrt{\epsilon})$ when the trajectory passes in the vicinity of a saddle point. On the other hand, the total orbital increment that can be computed by integrating Eq. (18) at constant p,q is $O(\sqrt{\epsilon})$, i.e., $\Delta p(q_0)=2\sqrt{\epsilon}I(q_0)$, where

$$I(q_0)=2\int_0^{3r}\frac{\xi\hat{G}(\xi;q,p)}{ry(\xi;q,p)}d\xi$$
$$\approx\frac{2}{r_0}\int_0^{3r_0}\frac{\hat{G}(\xi;q_0,0)}{\sqrt{r_0-\xi/3}}d\xi\ . \tag{23}$$

This means that, under typical circumstances, the averaged equations adequately describe crossing the critical line $p=0$ separating regions of closed and unbounded orbits of the truncated system (8). One can envisage a situation when the hyperbolic branch can be separated into two subsets: Q^+, $I(q)>0$ at $q\in Q^+$; and Q^-, $I(q)<0$ at $q\in Q^-$. Then trajectories of the averaged system (16) leave the cusped region of closed orbits at $q\in Q^-$ and enter it at $q\in Q^+$, as sketched in Fig. 1(b).

Trajectories of the truncated system escape to infinity along the open integral curves. "Dissipative" terms in Eq. (7), however, increase along the way and match the "conservative" part at $x=O(\epsilon^{-1})$ and, respectively, $y=O(\epsilon^{3/2})$ and $z=O(\epsilon^{-2})$, i.e., when all variables become $O(1)$ on the original scale of Eq. (1) or (6). If, as assumed, the underlying system has no attractors away from the origin, any trajectory leaving the proximity of the origin after crossing the hyperbolic branch at some $q=q^-\in Q^-$ has to return elsewhere and reenter the domain of closed integral curves. This can be effected only by crossing the hyperbolic branch at some $q^+\in Q^+$. On the level of Eq. (16), this corresponds to a jump from $K^-=K(q^-),H^-=H(q^-)$ to $K^+=K(q^+),H^+=H(q^+)$ effected on an $O(1)$ time scale fast compared with the dissipative time scale $O(\epsilon^{-1/2})$. Now, if Eq. (16) has no attractors with the domain of closed integral curves, the trajectory returns to Q^- thus generating a one-dimensional map M_1: $Q^-\to Q^-$ or $Q^+\to Q^+$. A fixed point of this map corresponds to an attractor of the continuous system (7) that consists of a segment of a torus cut at both sides at a homoclinic cross section and tied up by a very long string extending into the region $x=O(\epsilon^{-1})$ and connecting hyperbolic points q^- and q^+ (a shape which suggests calling this attractor an "invariant necklace" rather than an invariant torus which it basically is).

Since the motion away from the origin is essentially three dimensional, the map M_1 is not necessarily inverti-

ble and, in principle, can generate chaotic behavior. Little else can be added; since the excursion into the large-amplitude region necessitates inclusion of higher-order terms of the nonlinearity in Eq. (1), the exact form of the map depends on a particular underlying system. The only specific effect associated with the crossing of the homoclinic branch is the anomalous intermittency phenomenon described by Fowler.[5] If, say, the system traverses a limit cycle corresponding to a fixed point of the map M_1 (i.e., an "invariant necklace" of the full system), it would sporadically undertake very rare [with a probability $O(\exp(-1/\sqrt{\epsilon}))$] irregular excursions away from the attractor. Similar rare effects would be superimposed on any chaotic attractor the map M_1 may possess.

V. MOTION IN THE PROXIMITY OF A HOMOCLINIC ORBIT

Analytically tractable small-amplitude chaotic motion can be detected in the case when the integrals H,K remain close to the hyperbolic branch, or, equivalently, $p=O(\epsilon)$. This can be realized if the integral $I(q_0)$ in Eq. (23) vanishes to the leading order at a certain q_0.

For this case, we shall construct a return map for the rescaled variables ϕ,ψ by matching the "inner" solution at $\xi=O(\sqrt{\epsilon})$ obtained in the preceding section with the "outer" solution valid at $\xi=O(1)$.

In the outer region, Eqs. (18) and (19) can be rewritten after substituting $p=\epsilon\phi$ and $q=q_0+\sqrt{\epsilon}\psi$ in the form

$$\frac{d\phi}{d\xi}=-\frac{\hat{G}(\xi;q_0+\epsilon^{1/2}\psi,0)}{\epsilon^{1/2}r\sqrt{r_0-\xi/3}(1+\epsilon^{1/2}d\psi/d\xi)}\ , \tag{24}$$

$$\frac{d\psi}{d\xi}=-\frac{\sqrt{r_0-\xi/3}}{\xi r_0^2}\hat{G}(\xi;q_0,0)\ . \tag{25}$$

As in the preceding section, it is convenient to set "initial" conditions $\phi=\phi^0$ and $\psi=\psi^0$ at the outer turning point $\xi=3r$; the radicals in Eqs. (24) and (25) have to be taken with the positive sign on the incoming branch and with the negative sign on the outgoing branch. The solution is to be matched with the inner solution (21) and (22) at $\xi=O(\epsilon^{1/2})$. Integrating Eq. (25) yields

$$\psi=\psi^0\pm\frac{1}{2c}\ln\left[\frac{1+\sqrt{1-\xi/3r_0}}{1-\sqrt{1-\xi/3r_0}}\right]\pm\psi_r(\xi)\ , \tag{26}$$

where

$$\psi_r=\frac{1}{c}(1-\sqrt{1-\xi/3})+\frac{1}{r_0^2}\int_{\xi}^{3r_0}(r_0-\xi'/3)^{1/2}\frac{\hat{G}(\xi';q_0,0)}{\xi'}d\xi' \tag{27}$$

denotes terms that do not diverge at $\xi\to 0$. The inner limit of Eq. (26)

$$\psi=\psi^0\mp(2c)^{-1}\ln(\xi/12r_0)\pm k_0\ , \tag{28}$$

where $k_0=\psi_r(0)$, is to be matched with the outer limit of Eq. (22)

$$\psi=\psi^i+\frac{1}{2c}\ln\left[\frac{4\epsilon^{-1/2}c\xi}{2c(\psi^i)^{1/2}\mp 1}\right] \tag{29}$$

to obtain the relation between ψ^i and ψ^0

$$\psi^i=\psi^0\mp\frac{1}{2c}\ln\left[\epsilon^{1/2}\frac{2c(\psi^i)^{1/2}+1}{48cr_0}\right]\pm k_0\ . \tag{30}$$

The upper sign corresponds to an orbital segment directed from the inner towards the outer turning point, and the lower sign, to an oppositely directed segment. The total round-trip change of ψ between two successive passings of the outer turning point is

$$\psi^0_{n+1}=\psi^0_n+\frac{1}{2c}\ln\left[\epsilon\frac{\psi^i-1/4c^2}{576r_0^2}\right]-2k_0\ . \tag{31}$$

Next, orbital changes of ϕ have to be computed by integrating Eq. (24). Straightforward expansion of the right-hand side (rhs) in $\epsilon^{1/2}$ would produce divergences at the outer turning point that are eliminated by introducing a strained coordinate $\zeta=\xi(1-\epsilon^{1/2}\psi/r_0)$. Then expanding Eq. (24) yields

$$\frac{d\phi}{d\xi}=\mp\frac{2\hat{G}(\zeta+\sqrt{\epsilon}\psi\zeta/r_0;q_0+\sqrt{\epsilon}\psi,0)[1+\sqrt{\epsilon}\psi/r_0-\sqrt{\epsilon}(1-\zeta/r_0)d\psi/d\xi]}{\sqrt{\epsilon}(r_0+\sqrt{\epsilon}\psi)(r_0-\zeta/3)^{1/2}(1+\sqrt{\epsilon}\psi/r_0)^{1/2}}$$
$$=\mp\frac{2\hat{G}(\zeta;q_0,0)}{\sqrt{\epsilon}r_0(r_0-\zeta/3)^{1/2}}+\psi(\zeta)F_1(\zeta)+F_2(\zeta)\ , \tag{32}$$

with

$$F_1(\zeta)=\frac{2}{r_0}(r_0-\zeta/3)^{-1/2}\left[\frac{\zeta}{r_0}\frac{\partial\hat{G}}{\partial\xi}+\frac{\partial\hat{G}}{\partial q}-\frac{\hat{G}}{2r_0}\right],$$
$$F_2(\zeta)=2r_0^{-4}\hat{G}^2(\zeta;q_0,0)(r_0/\zeta-1)\ , \tag{33}$$

where derivatives are evaluated at $\xi=\zeta$, $q=q_0$. When Eq. (32) is integrated from $\zeta=\epsilon^{1/2}\eta$ to $\zeta=3r_0$, the $O(\epsilon^{-1/2})$ term vanishes due to the condition $I=0$—see Eq. (23). The resulting inner limit of the outer solution is

$$\phi=\phi^0\pm c^{-1}\eta\mp k_1\psi^0+k_2\mp k_3\ , \tag{34}$$

with

$$k_1=\int_0^{3r_0}F_1(\zeta)d\zeta,\quad k_2=\int_0^{3r_0}F_2(\zeta)d\zeta\ ,$$
$$k_3=\int_0^{3r_0}\psi(\zeta)F_1(\zeta)d\zeta\ . \tag{35}$$

The outer solution for ψ, Eq. (26), should be used in the last integral. Matching with the outer limit of the inner solution (21)

$$\phi=\phi^i-\tfrac{1}{2}c^{-2}\pm c^{-1}\eta \tag{36}$$

yields

$$\phi=\phi^i\pm k_1\psi^0-\tfrac{1}{2}c^{-2}-k_2\pm k_3\ . \tag{37}$$

The overall change of ϕ between two successive passings of the inner turning point is

$$\phi^i_{n+1}=\phi^i_n-2k_1\psi^0_n-2k_3\ . \tag{38}$$

VI. NEXT-RETURN MAP

We have obtained a two-dimensional map, (31) and (38), with two variables changing in turn in such a way that their increments at each step depend on the current value of the other variable. Shifting and rescaling the variables

$$\phi^i=1/4c^2+Au,\quad \psi^0=k^{-1}(\tfrac{1}{2}Av+k_3)\ , \tag{39}$$

yields

$$\begin{aligned} u_{n+1}&=u_n+v_n\ ,\\ v_{n+1}&=v_n-C\ln u_{n+1}\ , \end{aligned} \tag{40}$$

where $C=k_1/Ac$. The parameter $A=576\epsilon^{-1}r_0^2e^{-4k_0c}$ is presumed to be $O(1)$; this just ensures that the orbital average $\langle\dot q\rangle$ vanishes in the leading order at $p=O(\epsilon)$.

The map (40) is area preserving, even though the continuous system it has been derived from is not conservative. The area-preserving property will be, generally, lost when higher terms in the above asymptotic expansion are taken into account. Abstracting for the time being from this weak dissipation (important as it may be) we can notice similarity to the well-known Chirikov map[6] that would be obtained if v is replaced by $k\sin v$ in the first, and $\ln u$ by $\ln|u|$ in the second equation. The common feature—logarithmic dependence of decrements of v on u—is, of course, not accidental, since both maps describe motion in the proximity of a homoclinic orbit.

The lack of periodicity in v bars the map (40) from sharing large-scale chaotic properties of the Chirikov map. The latter are most pronounced at $C\gg1$ when efficient phase-mixing makes decrements of u almost uncorrelated. In this case, repeated reinjection into the region where the Jacobi matrix of the map has a real eigenvalue outside the unit circle and the transformation is extensional generates chaotic trajectories that fill a finite region when the phase plane is wrapped onto a cylinder, i.e., v defined modulo 2π.

In our case large values of C are inadmissible since they would just cause prompt ejection into the region $u<0$ that corresponds to the runaway of trajectories of the underlying system to large amplitudes. Alteration of rotational and extensional transformations is also lacking. The map (40) is extensional at $u+v<C/4$, and, as numerical experiments confirm, trajectories straying into this region are eventually ejected across the axis $u=0$. The alternative is a trajectory confined to an invariant manifold lying entirely within the region where the Jacobi matrix has eigenvalues on the unit circle.

Within this region, while escape to large amplitude is prevented, trajectories generated by the map (40) retain the rich structure characteristic of area-preserving maps studied in connection with dynamics of nonintegrable Hamiltonian systems. Figure 2 shows successive magnifications of different trajectories at $C=0.296$. On the largest scale, one can see that invariant circles nested around the center at $u=1,v=0$ are destroyed at the periphery, and the principal resonance manifests itself in a crown of "petals," corresponding to a period-11 invariant circle. Under the magnification, the period-11 circles are seen, in their turn, exhibiting secondary resonances and breaking into higher-period circles. This picture is repeated, apparently *ad infinitum,* at still smaller scales. The magnified pictures exhibit particularly complex structures. In some parts, one observes a typical layering of invariant circles and resonances of different orders, as well as chaotic orbits passing near saddle points. In other parts, invariant circles and their resonances appear as islands in an escape region. Some orbits, represented by clouds of points, are in fact long chaotic transients and eventually escape across the line $u=0$.

The detailed structure of orbits is very sensitive to changes of the parameter C. Thus, the primary period-11 resonance in Fig. 2 disappears at $C=0.29$. On the other hand, a slight increase of C leads to consolidation of invariant circles encompassing the region of the primary resonance. Shifting the parameter to either side makes the structure of orbits on larger scales less sophisticated than in Fig. 2, and narrow resonance layers are observed only in the fringe peripheric belt bordering the escape region. Rich structure is recovered, however, in other parametric intervals, while the order of the primary resonance decreases with growing C. Thus, transitions in the interval $0.55<C<0.56$ resemble those in the interval $0.29<C<0.30$, but with the period-8 primary resonance instead of period-11.

The picture based exclusively on Eq. (40) should be amended by taking into account, first, reinjection of trajectories that escape beyond $u=0$, and second, small dissipative corrections to the map itself. The former is most likely to cause the trajectory, after a number of escapes, to be trapped in the rotational region. Small corrections violating the area preservation should play the most important role, as they either convert some (slightly distorted) invariant circles of Eq. (40) into attractors, or cause creation of chaotic attractors in the region of small-amplitude motion under the study. The latter is most likely to occur either within one of resonance shells of Eq. (40) or in the outer layer stabilized by compensating the extension by area contraction.

VII. CONCLUSION

The chaotic scenario emerging from the above picture can start and end as suggested by Fowler.[5] First, a stationary state situated on the elliptic branch of Eq. (10) surrenders stability to a periodic orbit via a supercritical Hopf bifurcation. This orbit subsequently expands as a

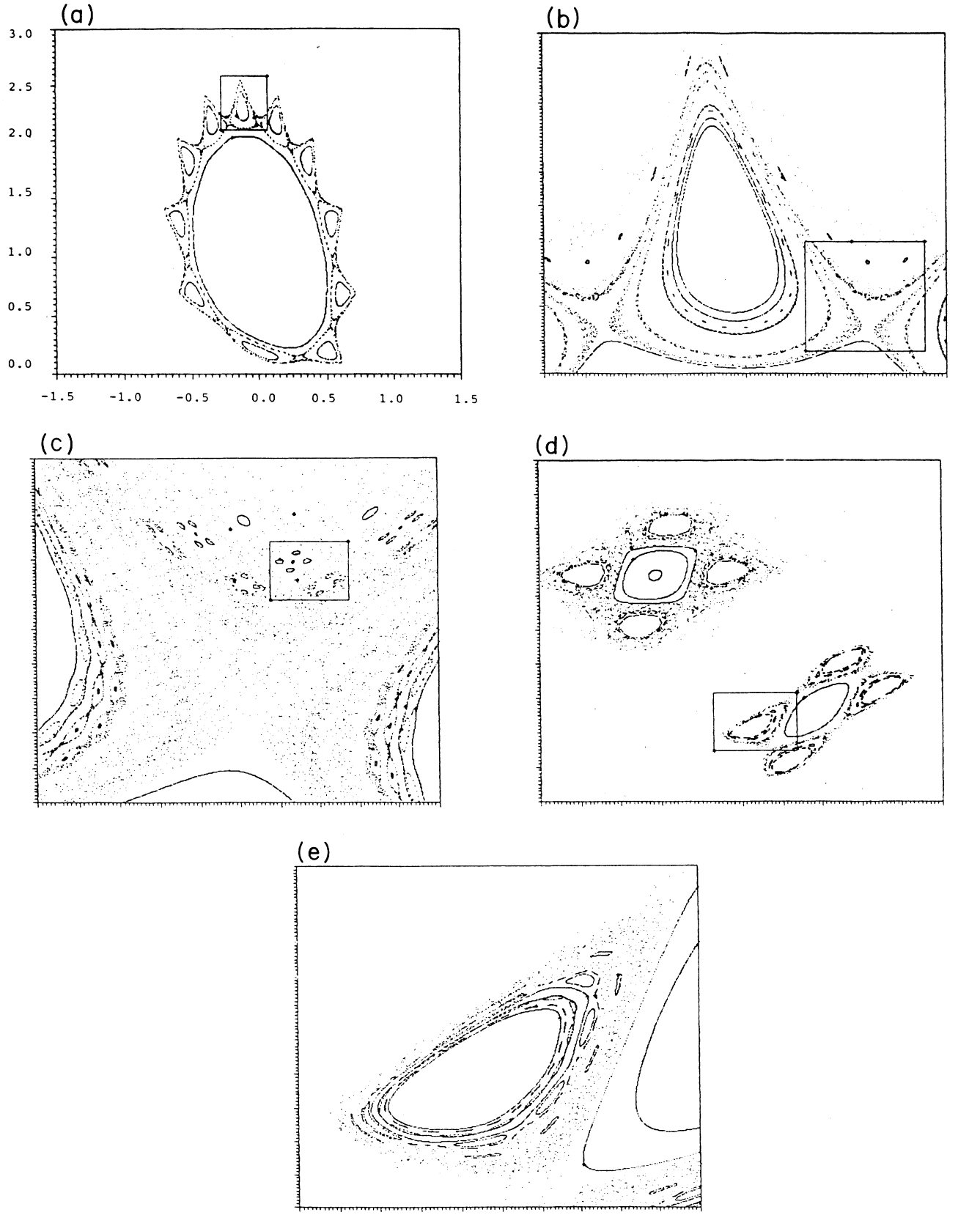

FIG. 2. Orbits (a) generated by the map (40) and their successive magnifications (b)—(e).

point representing the attractor of the averaged system traverses the cusped region in Fig. 1 towards the hyperbolic branch. Eventually, we find a situation when averaged equations have no attractors in the region of closed orbits and, as escape to infinity is not allowed, an attractor shaped as an invariant necklace has to be formed. In this state, the system spends most of the time spiraling around a toral segment represented by a path in Fig. 1(b) that connects some two points of the hyperbolic branch. In between, it undertakes swift excursions into the region of large amplitudes. The overall motion can be either quasiperiodic or chaotic depending on the properties of the map of the hyperbolic branch onto itself generated by the returning trajectory; nothing more definite can be said without exploring dynamics of a specific underlying system at large amplitudes. The only chaotic property of universal character one can observe is Fowler's anomalous intermittency manifesting itself in transcendentally rare events of ejection from the attractor.

The moment of transition between the small-scale periodic and large-scale necklace dynamics is most interesting, and it is near this point of "homoclinic explosion" where the richest variety of behavior can be observed. The logarithmic map (40) gives a most crude description of dynamics in the proximity of the hyperbolic branch. The area-preserving property of this map can be viewed as an undesirable accidental symmetry that precludes formation of small-amplitude attractors. On the other hand, the universal character of the map containing a single parameter helps to locate most sensitive areas where chaotic attractors are likely to appear when small dissipative corrections are brought in. We find such areas both in the internal resonance layer where the invariant circle undergoes repeated N-tupling and in the outer shell of nested invariant manifolds near the borderline between rotational and extentional motion.

Apparently, by tuning finely enough the parameters of Eq. (7), which influence both the parameter C and dissipative corrections, we could guide the system through different sequences of bifurcations on the way from the small-amplitude periodic motion to large-amplitude necklace dynamics, thus realizing any of an infinite number of routes to chaos that may exist, as emphasized by Holmes,[9] in systems described by two-dimensional maps. Different small-amplitude attractors encountered in this way can be possibly followed along appropriate paths in the parametric space of the underlying system away from the singular bifurcation point under study.

The above chaotic scenario is not the only one that is possible in the proximity of the bifurcation point at the triple-zero eigenvalue. As mentioned, formation of a homoclinic cycle of the averaged system (a feature shared with bifurcations of lower codimension) presents another alternative. The most straightforward transition from a stationary state to chaos can be brought about by moving a stable stationary state from the elliptic to the hyperbolic branch through the cusp at $q=-\alpha$; different scaling is required to probe dynamics near this point.

Though dynamics in the proximity of the cusp singularity at the triple-zero eigenvalue in no way exhausts the variety of three-dimensional motion, it is apparently rich enough to reflect the qualitative jump accompanying the transition from two to three dimensions. If two-dimensional dynamics, as reflected by dynamics in the proximity of a double-zero eigenvalue, involves only a finite number of distinct regimes and transitions, this number is apparently infinite in three dimensions.

ACKNOWLEDGMENT

The work has been supported by the US-Israel Binational Science Foundation.

APPENDIX: TRANSFORMATION TO THE NORMAL FORM

Let the quadratic part of Eq. (1) be presented as

$$f^i_{(2)}(x,y,z)=M^i_1x^2+M^i_2xy+M^i_3y^2+M^i_4xz+M^i_5yz+M^i_6z^2 \quad (i=1,2,3)\ . \tag{A1}$$

The quadratic transformation of the type (3) reducing (A1) to a normal form is

$$u_i\to u_i+P^i_1x^2+P^i_2xy+P^i_3y^2+P^i_4xz+P^i_5yz+P^i_6z^2 \tag{A2}$$

(with $u_1=x$, $u_2=y$, $u_3=z$). Using this in Eq. (1) yields the system of 18 equations for P^i_j

$$\begin{vmatrix} A & -\mathbb{1} & 0 \\ 0 & A & -\mathbb{1} \\ 0 & 0 & A \end{vmatrix} \begin{vmatrix} P^1_j \\ P^2_j \\ P^3_j \end{vmatrix} = \begin{vmatrix} M^1_j \\ M^2_j \\ M^3_j \end{vmatrix}\ , \tag{A3}$$

where $\mathbb{1}$ is the 6×6 unity matrix, 0 is the 6×6 block of zeros, and

$$A=\begin{vmatrix} 0&0&0&0&0&0 \\ 2&0&0&0&0&0 \\ 0&1&0&0&0&0 \\ 0&1&0&0&0&0 \\ 0&0&1&1&0&0 \\ 0&0&0&0&1&0 \end{vmatrix}\ . \tag{A4}$$

There is a number of alternative solutions of (A4) leading to 14 equivalent normal forms. The transformation we choose is

$$\begin{aligned} x&\to x+[\tfrac{1}{2}M^1_2+\tfrac{1}{6}(M^3_5+M^2_4+2M^2_3)]x^2 \\ &\quad+\tfrac{1}{3}(M^2_5+M^1_4+2M^1_3+M^3_6)xy\ , \\ y&\to y-M^1_1x^2+\tfrac{1}{3}(M^3_5+M^2_4+2M^2_3)xy \\ &\quad+\tfrac{1}{3}(M^1_4-M^1_3+M^2_5+M^3_6)y^2 \\ &\quad+\tfrac{1}{3}(2M^1_3-2M^1_4+M^2_5+M^3_6)xz-M^1_5yz-M^1_6z^2\ , \\ z&\to z-M^2_1x^2-(M^2_2+2M^1_1)xy+\tfrac{1}{3}(M^2_4-M^2_3+M^3_5)y^2 \\ &\quad+\tfrac{1}{3}(2M^2_3-2M^2_4+M^3_5)xz+M^3_6yz-(M^2_6+M^1_5)z^2\ , \end{aligned} \tag{A5}$$

yielding the normal form (4) with

$$\begin{aligned} &\mu_0=M^3_1,\ \ \mu_1=2M^2_1+M^3_2\ , \\ &\mu_2=2M^1_1+M^2_2+M^3_3,\ \ \mu_3=2M^1_1+M^2_2+M^3_4\ . \end{aligned} \tag{A6}$$

The coefficient of the cubic term $N_1^3 x^3$ originally present in the equation of z in (1) is transformed by (A5) to

$$\nu = N_1^3 - M_1^1 M_2^3 - M_1^2 M_4^3 + M_1^3 (M_2^1 + M_4^2) . \quad \text{(A7)}$$

The last term vanishes when $\mu_0 = M_1^3 = 0$.

For actual computation of coefficients of the unfolding (6) it is more convenient to use a simplified nonlinear transformation, taking the rhs of equations for the amplitudes x,y, respectively, as transformed amplitudes y,z. Since this is a near-identity transformation, it can be inverted perturbatively to the required order and then substituted into the equation of z. Nonlinear terms that are removed by (A5), but not by the simplified transformation, are of smaller order of magnitude and can be neglected; coefficients of other terms are identical to those generated by (A5).

[1]J. Guckenheimer and P. Holmes, *Nonlinear Oscillations, Dynamical Systems and Bifurcations of Vector Fields* (Springer, New York, 1983).

[2]A. Arneodo, P. H. Coullet and E. A. Spiegel, Phys. Lett. **92A**, 369 (1982); Geophys. Astrophys. Fluid Dyn. **31**, 1 (1985); A. Arneodo, P. H. Coullet, E. A. Spiegel, and C. Tresser, Physica D **14**, 327 (1985).

[3]L. M. Pismen, Chem. Eng. Sci. **40**, 905 (1985).

[4]J. B. Planeax, K. F. Jensen, and W. W. Farr, Lect. Appl. Math. **24**, 101 (1986).

[5]A. C. Fowler, Phys. Lett. **100A**, 1 (1984); Stud. Appl. Math. **70**, 215 (1984).

[6]B. V. Chirikov, Phys. Rep. **52**, 263 (1979).

[7]P. Glendinning and C. Sparrow, J. Stat. Phys. **35**, 645 (1984).

[8]T. Shimizu and A. Ichikawa, Phys. Lett. **91A**, 52 (1982).

[9]P. Holmes, Phys. Lett. **104A**, 299 (1984).